

1. Classification <i>INPE COM.4/RPE</i> <i>C.D.U.: 539.2: 535.33</i>		2. Period	4. Distribution Criterion	
3. Key Words (selected by the author) <i>PHOTOACOUSTIC</i> <i>SEMICONDUCTOR</i> <i>CdS</i>		internal <input type="checkbox"/>		external <input checked="" type="checkbox"/>
5. Report No. <i>INPE-2084-RPE/316</i>	6. Date <i>May, 1981</i>	7. Revised by <i>Ronald Ranvaud</i> <i>Ronald Ranvaud</i>		
8. Title and Sub-title <i>STUDY OF THE PHOTOACOUSTIC EFFECT IN SEMICONDUCTORS; EFFECT OF AN APPLIED DC- ELECTRIC FIELD.</i>		9. Authorized by <i>Nelson de Jesus Parada</i> <i>Nelson de Jesus Parada</i> <i>Director</i>		
10. Sector <i>DTE</i>	Code	11. No. of Copies <i>10</i>		
12. Authorship <i>I.N. Bandeira</i> <i>H. Closs</i> <i>C.C. Ghizoni</i>		14. No. of Pages <i>21</i>		
13. Signature of first author <i>Bandeira</i>		15. Price		
16. Summary/Notes <i>The photoacoustic spectroscopy of semiconductors is considered through a phenomenological approach, emphasizing carrier diffusion effects, enhanced by an applied electric field. Experimental results support the proposed model, and lead to the determination of various important semiconductor parameters.</i>				
17. Remarks <i>This paper will be submitted to Journal of Photoacoustics.</i>				

STUDY OF THE PHOTOACOUSTIC EFFECT IN SEMICONDUCTORS.
EFFECT OF AN APPLIED DC- ELECTRIC FIELD.

I.N. Bandeira, H. Closs, C.C. Ghizoni*
Conselho Nacional de Desenvolvimento Científico e Tecnológico
Instituto de Pesquisas Espaciais
12200 - S.J. dos Campos, SP, Brazil

ABSTRACT

The photoacoustic spectroscopy of semiconductors is considered through a phenomenological approach, emphasizing carrier diffusion effects, enhanced by an applied electric field. Experimental results support the proposed model, and lead to the determination of various important semiconductor parameters.

INTRODUCTION

The production of a photoacoustic (P.A.) signal in semiconductors involves intraband transitions of carriers photoexcited in the bulk, nonradiative bulk recombination, and nonradiative surface recombination of carriers generated within a diffusion length from the surface.

When optical absorption coefficients are high, heating is basically provided by surface recombination of excess carriers which are generated very close to the illuminated surface of the sample, so that transport properties of carriers are not relevant in describing the P.A. signal. In contrast to this case, carrier diffusion effects can play an important role in describing the production of the P.A. signal when optical absorption is low since a substantial fraction of photoexcited carriers is then generated in the bulk. However, the decrease in the P.A. signal which follows from the low light absorption prevents observation of diffusion

effects, and standard P.A. spectra of semiconductors are known to follow closely their optical spectra.

In order to enhance carrier diffusion effects at low absorption levels, a DC- electric field transverse to the light path can be applied to accelerate the charges generated, and thereby Joule-heat the sample. This is a clear bulk effect as opposed to the purely photoacoustic case where the surface plays the most important role in transferring thermal energy to the molecules of the gas filling up the cell.

It is the aim of this work to formulate a phenomenological approach to the P.A. effect in semiconductors including the effect of an applied DC- electric field which enhances the P.A. signal at wavelengths for which the absorption coefficient is low. The special features arising from this situation would allow the determination of important transport and optical parameters of semiconductors, such as recombination rates, surface recombination velocities and optical absorption coefficients at longwavelengths.

METHOD

The equations needed to describe the physical phenomenon are the thermal and charge diffusion equations. For the geometry of Figure 1, and following the notation of previous works^(1,2), the equations

$$\frac{\partial^2 \phi(x,t)}{\partial x^2} - \frac{1}{\alpha_s} \frac{\partial \phi(x,t)}{\partial t} = - \frac{p(x,t)}{K_s} \quad (1)$$

$$D \frac{\partial^2 n(x,t)}{\partial x^2} - \frac{n(x,t)}{\tau} - \frac{\partial n(x,t)}{\partial t} = - g(x,t) \quad (2)$$

describe the production of a temperature fluctuation $\phi(x,t)$ in the sample. In (1), $p(x,t)$ is the heat power density produced at a point \underline{x} inside the sample, α_s is the thermal diffusivity of the sample and K_s its thermal conductivity. In equation (2), $n(x,t)$ is the density of photoexcited carriers, D and τ are, respectively,

the diffusion constant and recombination time of the photoexcited carriers. The generation term $g(x,t)$ is given in terms of the light intensity $I(x,t)$ at the position \underline{x} inside the sample as $g(x,t) = \eta\lambda/hc \cdot \partial I(x,t)/\partial x$, with η being the quantum efficiency, λ the wavelength, h and c the Planck constant and the speed of the light, respectively. For a sinusoidally chopped monochromatic light beam incident in the semiconductor with an absorption coefficient β , the generation term assumes the form

$$g(x,t) = \frac{\eta\lambda\beta}{2hc} I_0 e^{\beta x} (1 + e^{i\omega t}) \quad (3)$$

with ω being the chopper angular frequency.

The heat density $p(x,t)$ produced at any point \underline{x} inside the sample is made up of various contributions, which are shown schematically in Figure 2. The different processes considered in the heat generation are:

1) Nonradiative thermalization of electrons with energy greater than E_g :

The heat power density is given as

$$\frac{dQ}{dt} = n_1(x,t) \cdot \frac{h\nu - E_g}{\tau_{IB}} \quad (4)$$

where $n_1(x,t)$ is the steady-state excess carrier concentration obtained from equation (2) neglecting diffusion effects, once the intraband relaxation time, τ_{IB} , is small ($\sim 10^{-12}$ sec.).

2) Joule heating

During a lifetime (τ_{BB}) in the conduction band, photoexcited electrons are accelerated by the external electric field applied perpendicularly to the diffusion direction. The heat density is therefore

$$\frac{dQ}{dt} = n_d(x,t) e\mu_n E^2, \quad (5)$$

where e , μ_n and E are, respectively, the electron charge, the

mobility and the applied electric field; $n_d(x,t)$ is the steady-state population of photoexcited carriers taking into account the diffusion processes. As the mobility of holes is very low compared to that of electrons, their Joule contribution is neglected.

3) Nonradiative bulk recombination:

After a diffusion length $L = \sqrt{D\tau_{BB}}$, excess electron-hole pairs recombine in the bulk, generating a heat power density given by

$$\frac{dQ}{dt} = \eta_B \cdot E_g / \tau_{BB} \cdot n_d(x,t) \quad (6)$$

where η_B is the fraction of the total energy E_g which is given up nonradiatively. This contribution exists only for photons with energy $h\nu$ greater than the band gap energy E_g .

4) Nonradiative surface recombination:

Excess carriers generated within a diffusion length ($\sqrt{D\tau_{BB}}$) from the surfaces recombine nonradiatively giving up a heat power density to the sample equal to

$$\frac{dQ}{dt} = \eta_s \cdot E_g [u_1 \delta(x) + u_2 \delta(x + \ell_s)] n_d(x,t) \quad (7)$$

where η_s is the fraction of E_g converted into heat and u_1 and u_2 are the surface recombination velocities at $x=0$ and $x=-\ell_s$, respectively. Finally, $\delta(x)$ is the Dirac's delta function.

Adding up the terms given in the expression (4) and (7), the heat power density of equation (1) is finally written as,

$$p(x,t) = \frac{h\nu - E_g}{\tau_{IB}} n_i(x,t) + \left\{ e\mu_n E^2 + \eta_B \frac{E_g}{\tau_{BB}} + \eta_s E_g [u_1 \delta(x) + u_2 \delta(x + \ell_s)] \right\} n_d(x,t) \quad (8)$$

The population $n_i(x,t)$ is obtained immediately as $n_i(x,t) = \tau_{IB} g(x,t)$.

In order to obtain $n_d(x,t)$, it is necessary to solve equation (2) subject to the boundary conditions imposed by the geometry of Figure 1. Surface recombination of excess carriers introduces discontinuities in the heat fluxes at the surfaces, which must be taken into account when solving equation (1) for $\phi(x,t)$.

Solutions to equation (1) and (2) are obtained in a tedious but straightforward way. The pressure fluctuation inside the P.A. cell is obtained from $\phi(x,t)$ as in reference 1, and is presented in the appendix. To account for the finite linewidth of the light source, the final expression should be averaged over the monochromator spectral bandwidth, a procedure which has not been attempted in this paper.

A sample of Cadmium Sulfide, 5 x 5 mm by 1 mm thick was chosen to verify the present model. Indium electrodes were evaporated as shown in Figure 1, and the sample was placed in a Photoacoustic Cell with a transparent support in order to allow transmission measurements. The light from a 1 kW xenon-lamp was chopped and focussed into the entrance slit of a monochromator. The monochromator light was focussed into the P.A. cell and the light transmitted throughout the sample measured by a pyroelectric detector. The experimental set-up is presented schematically in Figure 3. With this arrangement, the P.A. signal with or without a DC- electric field, and the transmission coefficient were measured simultaneously. The current flowing in the sample was also monitored.

RESULTS

With the experimental set-up described in last section, photoacoustic spectra of a CdS sample were obtained for various values of the applied voltage and chopper frequency (Figures 5 and 6). As an effect of carrier diffusion, the P.A. signal exhibits a peak whose intensity increases with increasing electric field. This maximum in the P.A. signal occurs at a wavelength for

which the absorption coefficient (β) is very close to the inverse of the carrier diffusion length (L) of the semiconducting sample. As the chopping frequency increases, approaching the carrier diffusion rate, the peak in the P.A. spectrum decreases relatively to the signal at high optical absorption wavelengths. The behaviours stated above can be explained by the fact that carriers generated within a diffusion length from the illuminated surface of the sample are less accelerated by the applied electric field, as surface recombination lowers their effective lifetime proportionally to their proximity to the surface; Joule heating is then negligible at high optical absorption coefficients. The effective lifetime becomes maximum for excess carriers which are generated at a depth equal or greater than L , so that for $\beta^{-1} > L$ a further decrease in β only decreases the total number of photoexcited carriers. Also the peak intensity is expected to decrease sharply with increasing chopping frequency, as less diffusion takes place before the light is turned off. The transmitted light (T), measured with a pyroelectric detector, did not change with the applied electric field. It is presented in Figure 4 together with the absorption coefficient (β). Values of β for wavelengths up to $\lambda = 520$ nm were taken from the literature⁽³⁾ while those of low light absorption ($\lambda > 520$ nm) were adjusted so that the theoretical curves fit the experimental results.

DISCUSSION

The agreement between the experimental results and the theoretical results predicted by the model, is quite apparent from Figures 5, 6 and 7,8. The experimental spectrum present a peak broader than the theoretical one, due to the finite line-width of the light source which was not taken into account. The enhancement of the P.A. signal at the region of low absorption allows the determination of important parameters of semiconduc-

tors. One important parameter is the absorption coefficient (β) at wavelengths (λ) greater than the wavelength corresponding to the band gap. The absorption in this region is usually very low and consequently difficult to measure by conventional ways. As an example, the absorption coefficient (β) for wavelengths greater than $\lambda = 520$ nm was roughly obtained by adjusting the theoretical P.A. spectrum to the experimental results (Figure 4). The determination of low absorption coefficients in semiconductors is one of the potential applications of the method just presented.

The presence of a well defined peak in the P.A. spectrum suggests a simple way to determine the carrier diffusion length. The maximum of the P.A. signal occurs for a β very close to the inverse of the diffusion length. This can be seen in the final expression for the P.A. signal (Appendix) by considering an expansion in β around $1/L$. The value of β which maximizes the P.A. signal is calculated to be, approximately

$$\beta_M \approx \frac{1}{L} [1 + (\omega \cdot \tau_{BB})^2]^{1/4} \quad (9)$$

For the case of CdS, with a chopper frequency of $\omega = 2\pi \times 20$ rad/s, the peak occurs at a wavelength $\lambda \approx 523$ nm ($\beta \approx 30 \text{ cm}^{-1}$). In this case $\omega \tau_{BB} \ll 1$ and the carrier diffusion length is calculated to be $L \approx 0.03$ cm. The peak for a chopper frequency of $2\pi \times 350$ rad/s occurs at a wavelength $\lambda \approx 521$ nm ($\beta \approx 50 \text{ cm}^{-1}$) and, with these values, the carrier diffusion lifetime is calculated to be $\tau_{BB} \approx 1 \times 10^{-3}$ sec.

The calculations described above are examples of the potentiality of the method in estimating parameters of semiconductor samples.

*Present address: EAV-IAE, Centro Técnico Aeroespacial
12200 S.J. dos Campos, SP, Brazil

REFERENCES

1. A. Rosencwaig and A. Gersho, Theory of the photoacoustic effect with solids, J.Appl.Phys. 47, 64 (1976)
2. J.P. McKelvey, Solid State and Semiconductor Physics (Harper & Row, New York, 1966), Chapter 10.
3. D.Dutton, Fundamental Absorption Edge in Cadmium Sulfide, Phys. Rev. 112, 785 (1958).

APPENDIX

When equation (2) is solved with the boundary conditions

$$D \frac{\partial n_d(x,t)}{\partial x} \Big|_{x=0} = -u_1 n_d(0,t)$$

and

$$D \frac{\partial n_d(x,t)}{\partial x} \Big|_{x=-\ell_s} = u_2 n_d(-\ell_s,t)$$

the AC component of $n_d(x,t)$ is obtained as

$$n_d(x,t) = \frac{\eta \lambda \beta \tau_{BB} I_o}{4 hc} \frac{e^{i\omega t}}{L^2 (m^2 - \beta^2)} \left\{ e^{\beta x} - A [B_1 \cosh(mx) + B_2 \sinh(mx)] \right\}$$

where

$$A = \frac{u_1 + \beta D}{m^2 D^2 + u_1 u_2 + m D (u_1 + u_2) \coth(m \ell_s)},$$

$$B_1 = m D \coth(m \ell_s) + u_2 + m D F,$$

$$B_2 = m D + u_2 \coth(m \ell_s) - u_1 F,$$

$$F = \frac{e^{-\beta \ell_s} (u_2 - \beta D)}{(u_1 + \beta D) \sinh(m \ell_s)},$$

and

$$m = \sqrt{1 + i\omega \tau_{BB}} / L$$

In solving equation (1), we have used the same boundary conditions of reference 1, except for the discontinuities introduced in the heat flux at the gas-semiconductor and semiconductor-backing interfaces, due to the heat generated by surface recombination of excess carriers:

$$K(x) \frac{\partial^2 \psi(x,t)}{\partial x^2} = \rho(x) C(x) \frac{\partial \phi(x,t)}{\partial t} -$$

$$- \eta_s E_g H n_d(x,t) [\delta(x) + \delta(x + \ell_s)]$$

here $K(x)$, $\rho(x)$, $C(x)$ and $u(x)$ are respectively the thermal conductivity, mass density, specific heat and surface recombination velocity at the points $x=0$ and $x=-\ell_s$;

$$H = 1 \text{ if } h\nu > E_g \text{ and } H = 0 \text{ if } h\nu < E_g.$$

The final expression for the complex pressure fluctuation in the cell was then obtained as

$$\delta P(t) = \frac{\gamma P_o I_o \eta \lambda \beta}{2\sqrt{2} T_o K_s \ell_g a h c} \cdot \frac{e^{i(\omega t - \pi/4)}}{R} \left\{ \frac{(h\nu - E_g) H}{1 + i\omega\tau_{IB}} \cdot \frac{S}{\beta^2 - \sigma_s^2} + \right.$$

$$\left. + \frac{\eta_B E_g H + \mu_n E^2 \tau_{BB}}{L^2 (m^2 - \beta^2)} \left[\frac{S}{\beta^2 - \sigma_s^2} - \frac{Y}{m^2 - \sigma_s^2} \right] + \frac{\eta_s E_g H \tau_{BB}}{L^2 (m^2 - \beta^2)} W \right\},$$

where

$$R = (g + 1)(b + 1)e^{\sigma_s \ell_s} - (g - 1)(b - 1)e^{-\sigma_s \ell_s},$$

$$S = (b + 1)(r - 1)e^{\sigma_s \ell_s} - (b - 1)(r + 1)e^{-\sigma_s \ell_s} - 2(b - r)e^{-\beta \ell_s},$$

$$Y = A \left\{ (b + 1)(tB_2 - B_1)e^{\sigma_s \ell_s} - (b - 1)(tB_2 + B_1)e^{-\sigma_s \ell_s} + \right.$$

$$\left. + (b + t)(B_1 - B_2)e^{m \ell_s} + (b - t)(B_2 + B_1)e^{-m \ell_s} \right\},$$

$$W = \frac{1}{\sigma_s} \left\{ u_1 \left[(b + 1)e^{\sigma_s \ell_s} - (b - 1)e^{-\sigma_s \ell_s} \right] - 2u_2 e^{-\beta \ell_s} + \right.$$

$$\left. + A \left[u_2 \left\{ (B_1 - B_2)e^{m \ell_s} + (B_1 + B_2)e^{-m \ell_s} \right\} - u_1 B_1 \left\{ (b + 1)e^{-\sigma_s \ell_s} - \right. \right. \right.$$

$$\left. \left. - (b - 1)e^{-\sigma_s \ell_s} \right\} \right] \right\}$$

and

$$c_s = a_s (1 + i)$$

$$a_i = (\omega/2 \alpha_i)^{1/2}, \quad i = g, s, b$$

$$r = \beta/\sigma_s$$

$$t = m/\sigma_s$$

where r , P_o ; T_o , g , s and b have the same meaning as in reference 1.

The theoretical curves in Figures 7 and 8 were obtained using the following parameters:

a- Thermal parameters

$$\alpha_s = 0.153 \quad \alpha_g = 0.247 \quad \alpha_b = 0.012$$

$$K_s = 0.272 \quad K_g = 0.00026 \quad K_b = 0.063$$

where α_i (in cm^2/sec) is the thermal diffusivity and K_i (in $\text{W}/\text{cm}\cdot\text{K}$) is the thermal conductivity. The subscript i refers to the medium: s for solid (CdS); g for gas (air); b for backing (lucite).

b - Transport parameters

. Diffusion constant

$$D^* = \frac{2D_p D_n}{D_p + D_n} \approx 2 D_p = 1.0 \text{ cm}^2/\text{sec}$$

where D_p (holes) = $0.5 \text{ cm}^2/\text{sec}$ and D_n (electrons) = $9.0 \text{ cm}^2/\text{sec}$.

. Surface recombination velocity

$$u_1 = u_2 = 10^4 \text{ cm/s (front and back surface)}$$

. Lifetimes

$$\tau_{1B} = 10^{-12} \text{ sec}, \quad \tau_{2B} = 10^{-3} \text{ sec.}$$

. Process efficiencies

$$\eta_s = \eta_b = 1$$

where s and b refer to surface and bulk respectively.

. Electron mobility

$$\mu_n = 350 \text{ cm}^2/\text{V}\cdot\text{sec.}$$

FIGURE CAPTIONS:

- Figure 1: CdS sample with indium contacts subjected to radiation and electric field.
- Figure 2: Heat generation processes in semiconductor photoacoustics (see text).
- Figure 3: Experimental set-up for measurements of P.A. signal.
- Figure 4: Optical absorption (β) and transmission (T) curves of CdS sample. β full curve is from reference 3 and dotted is predicted by the present model.
- Figure 5: Experimental results of CdS sample for various values of electric fields with a chopped frequency of 20 Hz.
- Figure 6: Experimental results of CdS sample for two values of chopper frequency and a fixed 16 V/cm electric field applied.
- Figure 7: Theoretical curves for CdS with various applied electric fields and a frequency of 20 Hz. For the other parameters used see appendix.
- Figure 8: Theoretical curves of CdS for two frequencies. The electrical field is 16 V/cm and the other parameters used are in the appendix.

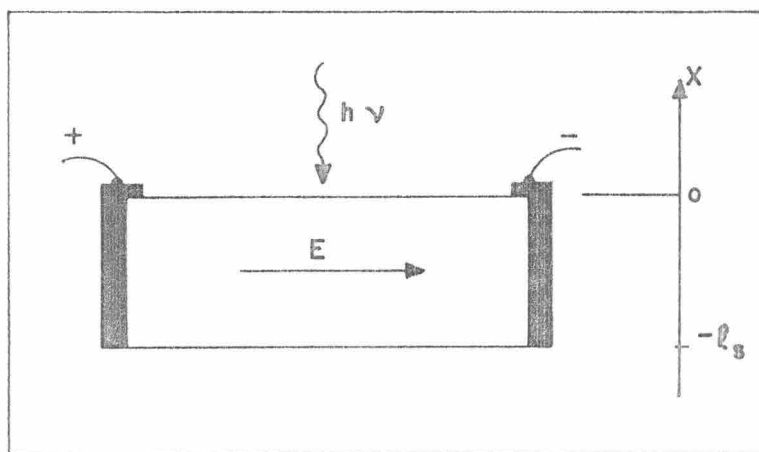


Fig. 1.

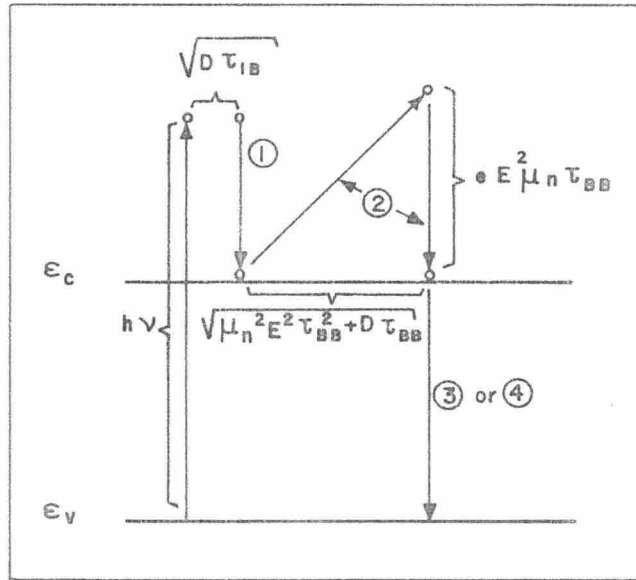


Fig. 2

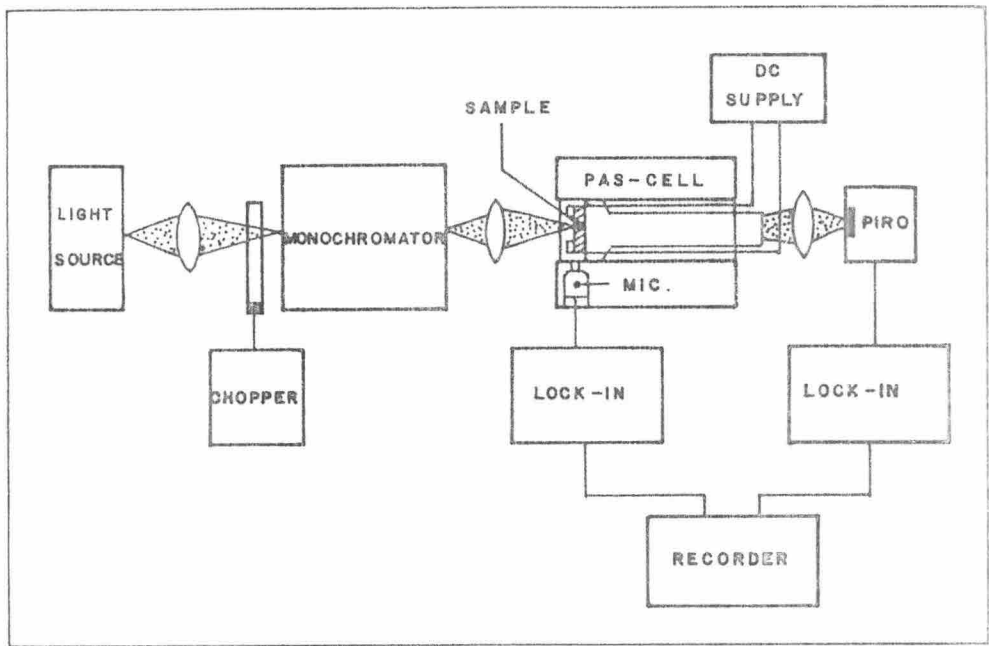


Fig. 3.

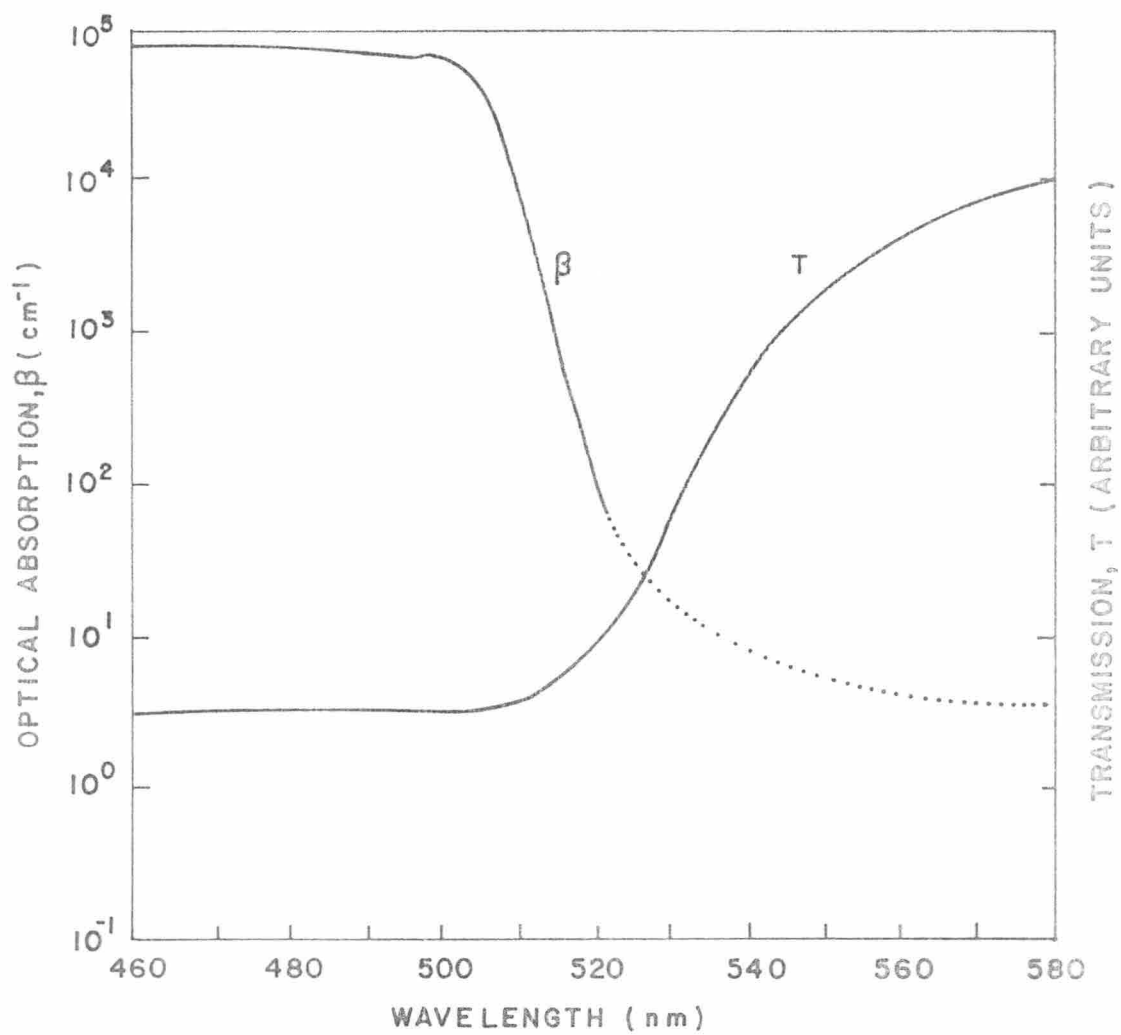


Fig. 4.

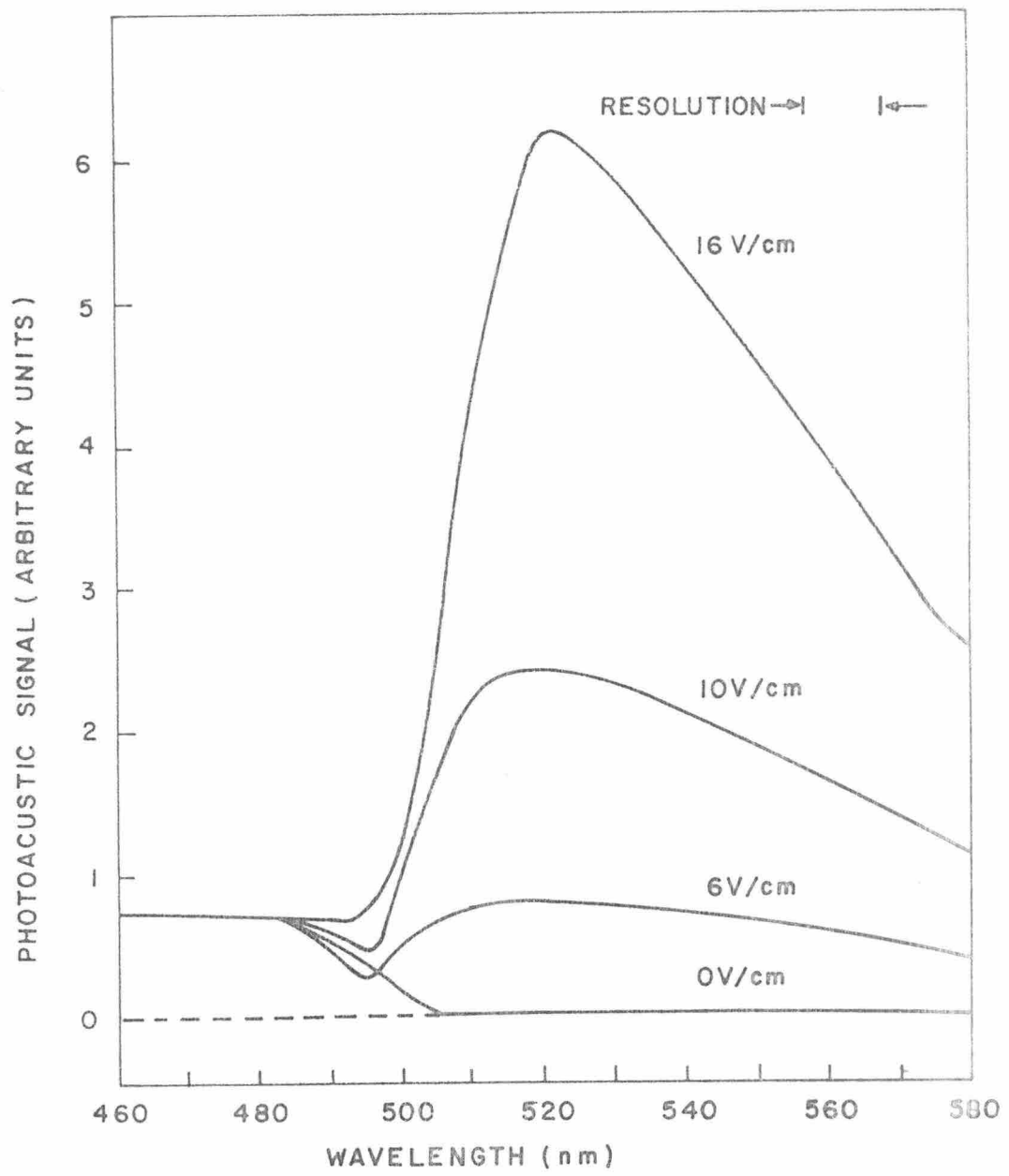


Fig. 5.

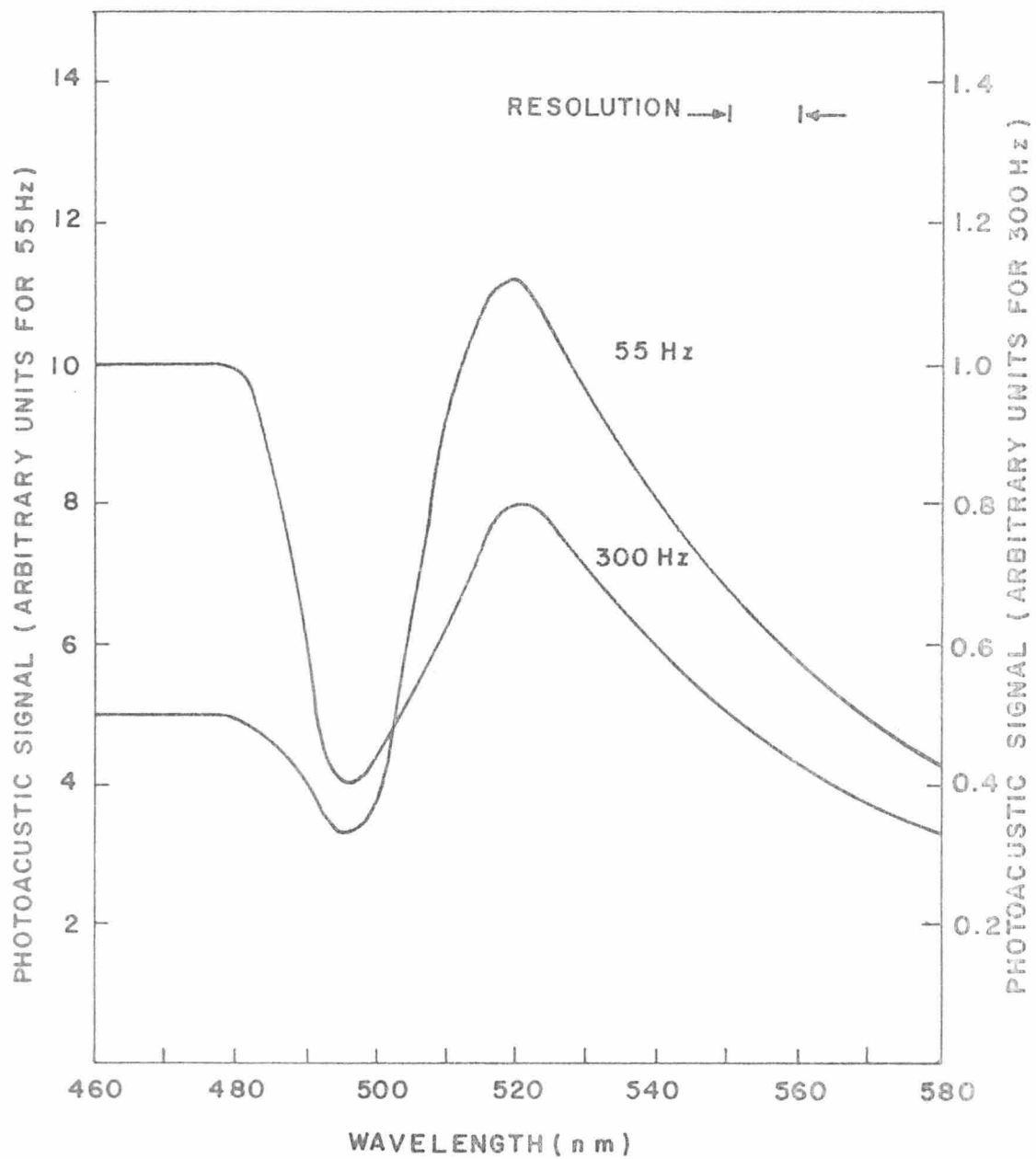


Fig. 6.

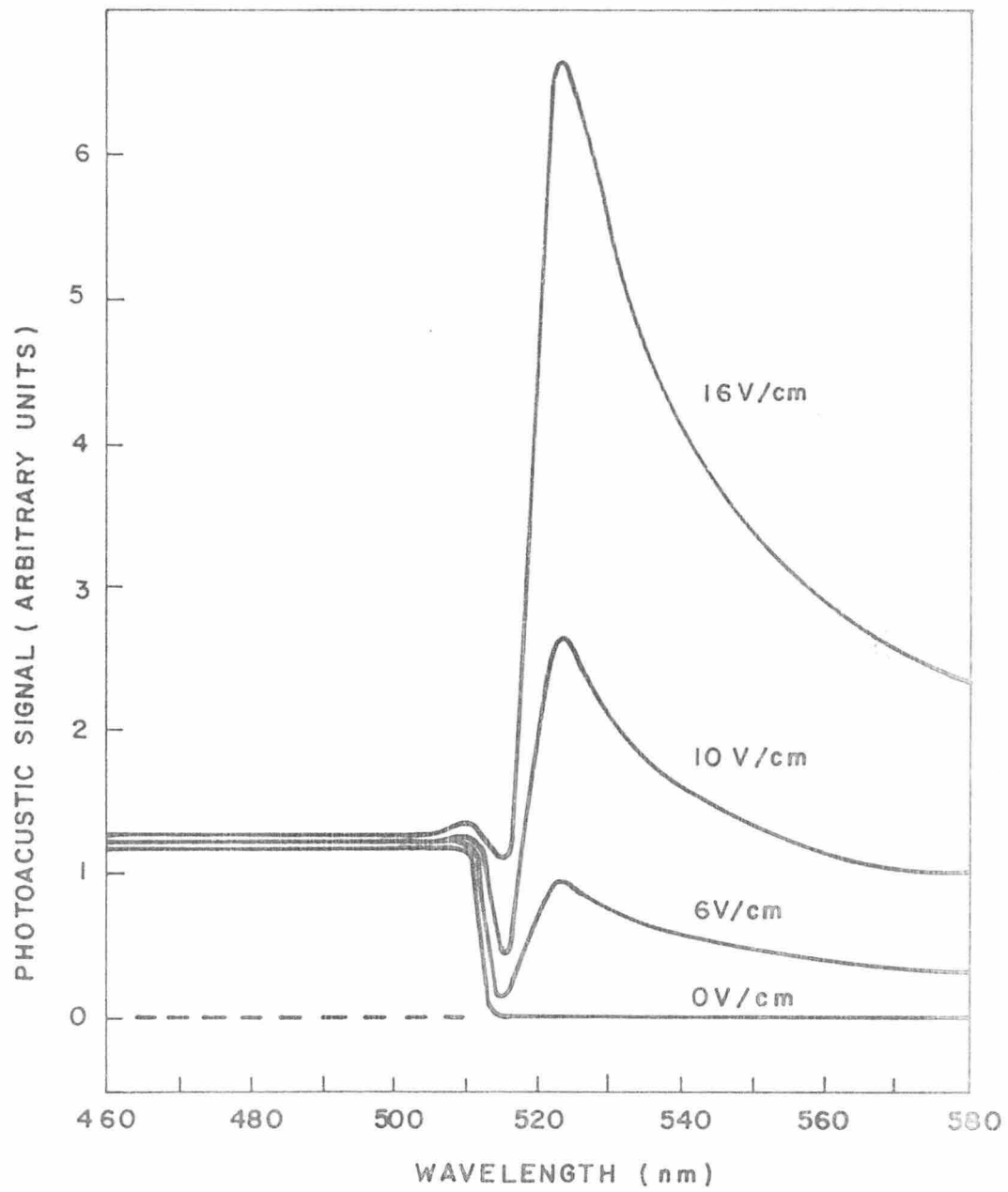


Fig. 7.

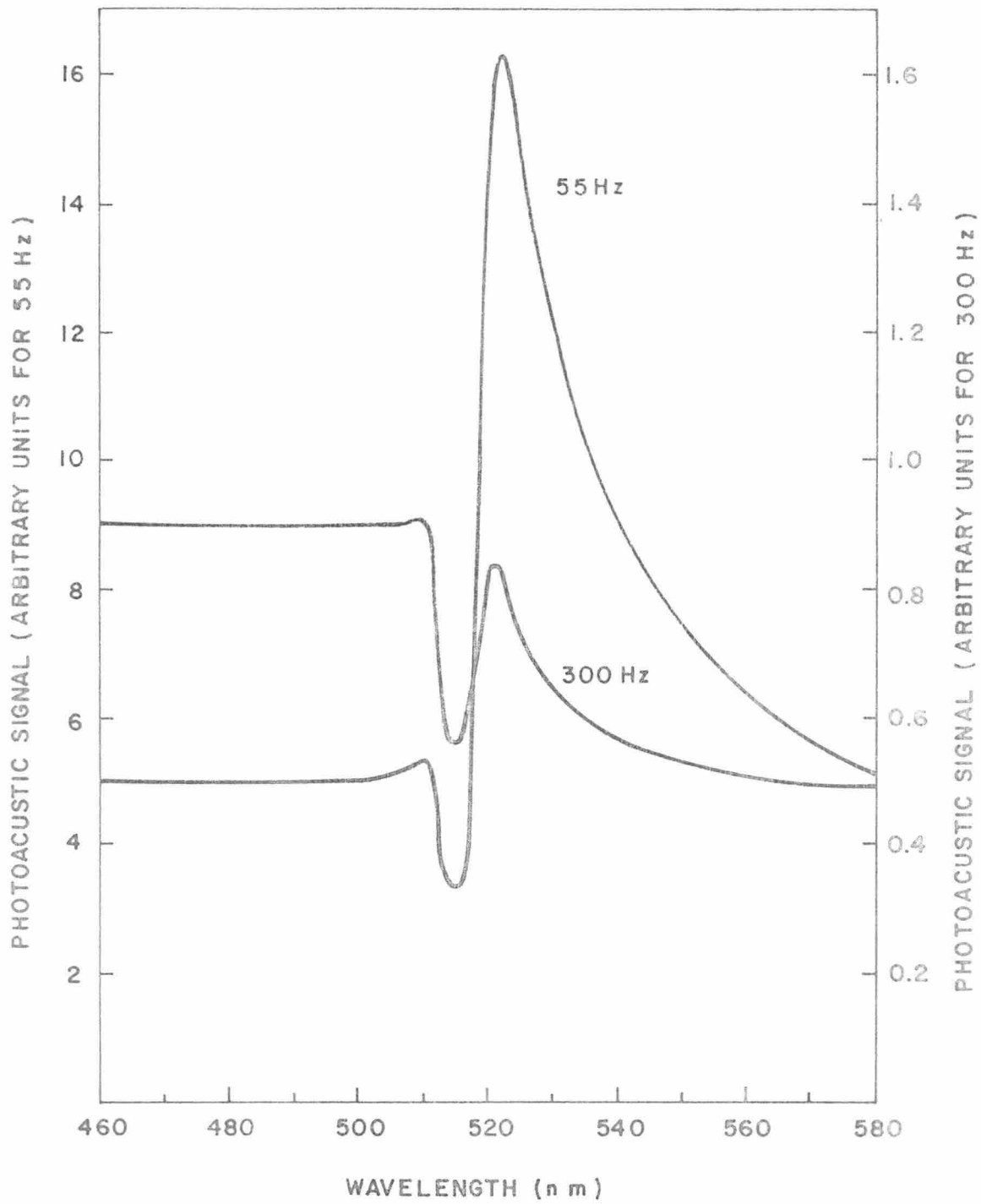


Fig. 8.